Bridging Iterative Ensemble Smoother and Multiple-Point

Geostatistics for Better Flow and Transport Modeling

Zhendan Cao^a, Liangping Li^{a,*}, Kang Chen^b

^aDepartment of Geology and Geological Engineering, South Dakota School of Mines and Technology, Rapid City, 57701, USA

^bSchool of Water Resources and Environment, Hebei GEO University, Shijiazhuang, 050031, China

Abstract

Inverse method can be used to fill the gap between huge amount of data from sensors and complex

groundwater model. The iterative Ensemble Smoother (iES) is one of the most efficient algorithms applied to

groundwater modeling for data assimilation. However, the iES only works for multi-Gaussian fields, because

two-point statistics are used to estimate the co-relation between state variables and parameters. In curvilinear

geometries, such as sinuous channels in fluvial deposits, the distribution of hydraulic conductivity is non-

multiGaussian. Multiple-Point Geostatistics (MPG) method has gained popularity for modeling curvilinear

structures by conditioning on directly measured data, such as conductivities. This paper is aimed at bridging

the iES and MPG method via pilot points to deal with inverse problem for further conditioning on indirect

data, such as piezometric head, in non-Gaussian fields. As a result, the better flow and transport modeling

will be achieved because both data and the concept model (e.g., geological structures) are honored after data

assimilation. To do that, the iES is used to update conductivities at pilot points by assimilating indirect

data, then the updated values at pilot points together with measured conductivities will be used as hard

data to model hydraulic conductivity field via Direct Sampling, an MPG method. A synthetic example was

used to demonstrate the methodology in terms of characterization of conductivity and flow and transport

predictions. The results show that this new approach can not only assimilate dynamic data into groundwater

flow model but also preserve curvilinear structures.

Keywords: Inverse Modeling, Iterative Ensemble Smoother, Pilot Point, Direct Sampling

1. Introduction

Accurate characterization of the spatial variation of hydrological properties such as hydrologic conduc-

tivity and their corresponding uncertainty is a key issue for a range of engineering problems such as site

*Corresponding author

Email address: liangping.li@sdsmt.edu (Liangping Li)

remediation and restoration, waste disposal for radioactive material and carbon sequestration for mitigating greenhouse gas emission (e.g., Rabideau and Miller, 1994; De Marsily et al., 2005; Lengler et al., 2010).

In the framework of Monte-Carlo simulation, there are two steps that are routinely used to characterize the
heterogeneity of hydraulic conductivity in groundwater studies, using direct and indirect measurements from
the field. First, directly measured hydraulic conductivities, normally termed as hard data, can be conditioned
through geostatistical approaches, such as Sequential Gaussian Simulation (Deutsch and Journel, 1992;
Gómez-Hernández and Journel, 1993) and multiple-point geostatistics (Strebelle, 2002). Second, indirect
head and concentration data, termed as soft data, can then be further conditioned through inverse methods
in groundwater modeling (e.g, Hendricks Franssen, 2001; Zhou et al., 2014).

Inverse method is an approach to calibrate initial parameters by minimizing an objective function that is generally composed of the sum of squared difference between observed indirect data and simulated values. The initial parameters are iteratively adjusted through a gradient-based approach or posterior sampling. Examples of these inverse methods include pilot point method (RamaRao et al., 1995), self-calibration method (Gomez-Hernandez et al., 1997), the Markov chain Monte Carlo method (Oliver et al., 1997), and gradual deformation (Hu, 2000). A comprehensive review of inverse methods can be found from the literature (e.g., Yeh, 1986; Hendricks Franssen et al., 2009; Zhou et al., 2014).

Comparing with inverse methods mentioned above, the Ensemble Kalman Filter (EnKF) has increasingly gained popularity because of its CPU-efficiency and ease of implementation (Hendricks Franssen and 21 Kinzelbach, 2009; Xu et al., 2013). The EnKF was first introduced by Evensen (1994) and widely applied to 22 a spectrum of fields such as groundwater modeling, petroleum engineering, weather forecast and oceanography. Reichle et al. (2002) applied the EnKF to estimate soil moisture by assimilating L-band (1.4 GHz) microwave radio-brightness observations into a land surface model. Different ensemble sizes were tested in terms of the efficiency of the EnKF, using a series of synthetic experiments. The results indicate that the EnKF is an efficient data assimilation approach in land surface modeling for moderate ensemble size. Chen 27 and Zhang (2006) applied the EnKF to update hydraulic conductivities by integrating observed hydraulic head data for a transient groundwater flow model in geologic formations. A two-dimensional example and a three-dimensional example were used to test the capability of the EnKF and the results show that the EnKF could provide an efficient approach for the estimation of hydraulic conductivity. Gu et al. (2005) 31 applied the EnKF to calibrate permeability using history pressure data in a reservoir model, and concluded that the EnKF can provide a faster computational speed and a reliable estimation of parameters in the synthetic example. Liu et al. (2008) applied the EnKF to inversely calibrate the hydraulic conductivity and

transport parameters such as dispersivity using hydraulic head and tracer concentration data at the MADE site. Huang et al. (2009) used the EnKF to assimilate both hydraulic head and solute concentration data to update the hydraulic conductivity field in order to get a better prediction of solute transport. Kurtz et al. (2014) employed the EnKF to jointly assimilate piezometric head data and groundwater temperature for updating river bed conductivity in a river-aquifer model. Li et al. (2017) used both surface deformation and hydraulic head to calibrate the transmissivity and elastic/inelastic specific storages via the EnKF and a synthetic example shows that the EnKF can effectively reduce model uncertainty after conditioning on all the data in a land subsidence model.

An alternative data assimilation method to the EnKF is the Ensemble Smoother (ES), which was first

presented by van Leeuwen and Evensen (1996) and has been emerged as an effective and efficient approach for
data assimilation. The analysis scheme of the ES is similar to the EnKF. However, in ES, all the observation
data are assimilated at once to update the state parameter instead of assimilating observations sequentially
in the EnKF. Because there is no recurring groundwater modeling, the ES has much less computational cost.

Bailey and Baù (2010) applied the ES to calibrate the hydraulic conductivity by assimilating hydraulic head
and return flow volume. Bailey et al. (2012) used the ES to improve the estimation of denitrification rate
by assimilating nitrate concentration and nitrate mass data. In order to improve the method and to avoid
the impact of strong non-linearity of the forward simulator, an iterative ES (iES) was proposed, in which
the same set of data is iteratively applied to update parameters. Li et al. (2018a) compared the EnKF and
the iterative ES, and found that the latter can achieve similar results as the EnKF but have an advantage
of less computational cost.

Although the EnKF/iES has been extensively applied in subsurface flow models, it only performs well in aquifers where the hydraulic conductivity follows a multiGaussian distribution. In curvilinear structures such as fractures in sedimentary rocks and channels in fluvial deposits, the hydraulic conductivity does not have the multiGaussian distribution. Multiple Points Geostatistics (MPG) method has been widely used to simulate the non-multiGaussian geological deposits in the past decades. Instead of using two-point variogram-based geostatistics, MPG uses multiple-point (e.g., pattern) to represent correlations of multiple variables in space. Strebelle (2002) proposed a Single Normal Equation simulation(SNESIM) method to model the curvilinear structure using a training image. The training image is a conceptual model which is composed of the potential structures of the target aquifer. One of shortcomings for SNESIM is that: it can only model categorical variables such as rock facies. However, aquifer parameters such as hydraulic conductivity and porosity in groundwater modeling are continuous variables. More recently, Mariethoz et al.

(2010) developed a Direct Sampling (DS) method to simulate the geological curvilinear structures. It can not only model categorical variables but also continuous variables, and has an advantage of less computational cost.

Although there is a wide range of methods to simulate the non-multiGaussian geological fields through MPG methods, it is a challenge to conditioning on indirect data such as hydraulic head data for improved 70 flow and transport predictions. Caers (2003) proposed a probability perturbation method to solve the inverse problem by updating MPG realizations simulated by SNESIM, using a Markov chain process until all observation data match simulated ones. Sarma et al. (2009) applied a kernel-based generalized EnKF to update 73 permeabilities in non-Gaussian reservoirs. However, the back transformation calculation is still a challenge to solve. Zhou et al. (2011) presented a normal-score EnKF method, where the non-Gaussian distributed log-conductivity was transformed into the Gaussian distributed log-conductivity before implementing the EnKF, in order to handle the non-Gaussianity. Li et al. (2018b) developed an iterative normal-score Ensemble Smoother using the same method to deal with non-Gaussianity in data assimilation. Zhou et al. (2012) developed a pattern-search-based method based on the idea of DS method. Instead of just searching the hydraulic conductivity pattern, the corresponding hydraulic head pattern is also included as a part of ensemble pattern search. Li et al. (2013) proposed an ensemble PATtern (EnPAT) search method as an extension to the pattern-search-based method by simultaneously updating both hydraulic conductivity and hydraulic head, and an improved characterization of patterns is achieved in a synthetic example for groundwater modeling. 84

In this paper, we propose a new approach to address the inverse problem of MPG simulations, by coupling iterative ES and Direct Sampling method. Specifically, a set of pilot points are chosen randomly from the hydraulic conductivity field. Then, they will be updated using dynamic data (i.e., observation head) via iterative ES. The updated conductivities at pilot points will be regarded as hard data to interpolate the hydraulic conductivity fields at un-sampled locations using DS in order to preserve geological structures that are displayed in the concept model (i.e., training image). The proposed approach can not only efficiently assimilate dynamic data into groundwater modeling through the iES, but also preserve the non-multiGaussian feature through DS. The coupled iES-DS method is built on the iterative ES in assimilating dynamic data and on DS in modeling non-multGaussian fields. The proposed method will be demonstrated in a synthetic example, in terms of conductivity characterization and flow and transport predictions.

95 2. Methodology

96 2.1. Forward Modeling

The governing equation of groundwater transient flow in saturated porous media can be described as follows (Bear, 1972):

$$\frac{\partial}{\partial x} \left(K \frac{\partial h}{\partial x} \right) + \frac{\partial}{\partial y} \left(K \frac{\partial h}{\partial y} \right) + \frac{\partial}{\partial z} \left(K \frac{\partial h}{\partial z} \right) - W^* = S_s \frac{\partial h}{\partial t}$$
 (1)

where K is the hydraulic conductivity; h is the hydraulic head; S_s is the specific storage; t is time; and W^* is the source and sink.

The governing equation for the solute transport with linear equilibrium adsorption can be described by the following differential equation (Bear, 1972):

$$\nabla(\phi \mathbf{D} \cdot \nabla c) - \nabla \mathbf{q} c = \phi R \frac{\partial c}{\partial t}$$
 (2)

where c is solute concentration in the water phase; ϕ is the porosity; ∇ is the gradient operator; \mathbf{D} is the local hydrodynamic dispersion coefficient tensor; \mathbf{q} is the Darcy velocity given by $\mathbf{q} = -K\nabla h$, and R is retardation factor.

106 2.2. Inverse Modeling

110

The proposed inverse method is based on the coupling of iterative ES and DS. A detailed explanation of iterative ensemble smoother can be found in van Leeuwen and Evensen (1996). Figure 1 is the flowchart of iES-DS, coupling with MODFLOW (Harbaugh et al., 2000). It can be summarized in following steps:

1. Build the joint vector:

$$\psi = \begin{bmatrix} lnK \\ h \end{bmatrix} \tag{3}$$

In this vector, K is the ensemble of log-hydraulic conductivities at pilot points, and h is the simulated heads after running MODFLOW. The i^{th} realization in this vector can be described as follows:

$$\Psi_{i} = \begin{bmatrix}
(lnk_{1}, & lnk_{2}, & \cdots, & lnk_{m})^{T} \\
(h_{1}, & h_{2}, & \cdots, & h_{n})_{1}^{T} \\
(h_{1}, & h_{2}, & \cdots, & h_{n})_{2}^{T} \\
(\vdots & \vdots & \vdots & \vdots) \\
(h_{1}, & h_{2}, & \cdots, & h_{n})_{k}^{T}
\end{bmatrix}_{i}$$
(4)

where m denotes the number of pilot points; n denotes the number of nodes where hydraulic heads are collected; k denotes the number of time step; and T is the transpose matrix symbol. Unlike the EnKF, all simulated hydraulic head data at all time steps are jointed globally in the iES.

2. Calculate the error covariance for the predicted state:

$$\boldsymbol{P}_{e}^{f} = \frac{1}{N_{e} - 1} \sum_{i=1}^{N_{e}} (\boldsymbol{\psi}^{f} - \overline{\boldsymbol{\psi}}^{f}) (\boldsymbol{\psi}^{f} - \overline{\boldsymbol{\psi}}^{f})^{T}$$

$$(5)$$

where f denotes the forecast state. The overline denotes the mean of the forecast ensemble. The mean of ensemble is used to represent the best estimate of the true value. N_e denotes the number of realizations in the ensemble. Broadly, more realizations will provide a more accurate estimation of cross-covariance, but need a higher computational cost accordingly.

3. Calculate the Kalman Gain.

The Kalman gain is a weight coefficient matrix and used to adjust the forecast matrix by minimizing the error between observation data and simulations. d is an ensemble of observations with an error ϵ_i for the ith realization. d_i is an observation vector including the true piezometric heads d and observation error ϵ_i .

$$d_i = d + \epsilon_i \tag{6}$$

 R_e is the ensemble error covariance:

$$R_e = \overline{\epsilon \epsilon^T} \tag{7}$$

Kalman Gain can be written as,

$$K_e = P_e^f H^T (H P_e^f H^T + R_e)^{-1}$$
(8)

where \boldsymbol{H} is the measurement matrix.

4. Update the ensemble by the following equation:

129

130

131

132

$$\psi_i^a = \psi_i^f + K_e(d_i - H\psi_i^f) \tag{9}$$

where ψ_i^a is the updated realizations and ψ_i^f is the forecast realizations.

- 5. Interpolate both the updated hydraulic conductivities at pilot points and hard data to un-sampled locations, using DS method. The algorithm of the DS is described in detail in Mariethoz et al. (2010).
- 6. Go back to Step 1 until the mismatch of hydraulic heads converges. Emerick and Reynolds (2013) discussed a set of termination criteria that can be used for the iterative ES.

Note that, the concept of pilot points plays a key role in the proposed methodology and it connects
the iES and DS for handling the inverse problem of non-Gaussian fields. If no pilot points are considered,
the coupled iES-DS comes to the DS alone. In other words, dynamic data will not be integrated into the
MPG simulations. On the other hand, if all the nodes are pilot points, the proposed algorithm becomes the
iES, and the non-Gaussian features can not be preserved after data assimilation. The pilot points bridge
the iterative ES and DS for dealing with non-Gaussianity in data assimilation for better flow and transport
modeling.

3. A Synthetic Example

A synthetic example is designed to test the performance of this new approach by coupling DS and iES 143 for data assimilation in a bimodal aquifer. A 2D transient flow model is considered. A time period of 30 days is divided into 60 time steps with a multiplier of 1.05. The aquifer has 50×50 cells and each cell has a 145 size of 5 m \times 5 m. The boundary conditions of the aquifer are simplified as no flow boundaries on the North and South sides and the East side is a constant head boundary (h = 5m). 50 pumping wells are set on the 147 west boundary. The pumping rate of these wells is set to $q = -3.0m^3/day$ at high conductivity cells and $q = -0.3m^3/day$ at low conductivity cells in order to get a prominent change of hydraulic heads at wells. 149 9 observation wells are used to get observed hydraulic head data for inverse modeling. Figure 2 shows the 150 schematic boundary conditions and the location of observation wells. Table 1 shows the setting parameters 151 for the synthetic example. MODFLOW (Harbaugh et al., 2000) is used to solve the flow equation (1). 152 DS method is used to generate the reference conductivity field (see Figure 3). The training image (Figure 153 4) is obtained by overlaying a continuous hydraulic conductivity field generated by Sequential Gaussian 154 Simulation (Gómez-Hernández and Journel, 1993), on a categorical facies field that has been routinely used 155

to test methodology in fluvial deposits (e.g., Li et al., 2015). The same training image is used to generate
the initial ensemble of conductivity fields via DS for integrating head data. Seven cases are considered with
different numbers of pilot points and ensemble size (see Table 2). The purpose of these cases is to validate
the method and to test the sensitivity of these key parameters to the results. Figure 5 shows the distribution
of pilot points and measured conductivities for Case 5.

4. Results and Discussion

4.1. Hydraulic Conductivity Characterization

Figures 6 and 7 show the ensemble mean and ensemble variance of conductivity fields for 7 Cases that are listed in Table 2.

For Case 1, no measured conductivities and head data are conditioned, and ensemble mean and ensemble variance of lnK tend to be constant, as expected. Although each individual realization, as the reference conductivity field in Figure 3, displays a strong heterogeneity with preferred flow paths, the averaging of conductivities through ensemble smears out those high permeable channels. In addition, since there are no measured hard and soft data that are considered, the ensemble variance that represents the uncertainty of hydraulic conductivity shows the highest.

For Case 2, six measured conductivities, as hard data, are conditioned through DS. Ensemble mean of conductivity fields displays a pattern that is close to the reference conductivity field in Figure 3, and overall ensemble variance is decreased, with zero variance at the locations of measured conductivities and gradually elevated variance away from the conditioning points.

For Case 3, besides the measured conductivities, head data collected from observation wells are used to update the conductivity ensemble of Case 2. The iterative ES is applied to update conductivities at all the nodes. In other words, all the nodes are pilot points, and thus no DS is used for interpolation. In terms of ensemble mean, the pattern is closer to the reference, compared with Case 2 where only measured conductivities are considered. Because additional head data are conditioned, ensemble variance is further decreased. However, because only two-point geostatistics (i.e., cross-covariances) are used, the pattern in each individual realization can not be preserved, which can be found in Figure 8 where the histogram of conductivity, after updating using iterative ES, has become a Gaussian distribution, departing from the bimodal distribution of the reference field.

In order to preserve the non-Gaussian feature (i.e., high permeable channels), a subset of nodes, terms as pilot points, is introduced. Specifically, the conductivities at pilot points are updated using head data via

iterative ES, and then DS is further used to extrapolate the updated conductivities at pilot points for other nodes. For Cases 4 - 6, the number of pilot points is gradually increased from 14 to 494, while the number of measured conductivities and hydraulic head data are kept the same. The ensemble size is 200 for these three Cases. The ensemble mean and ensemble variance is improved from Case 4 to 5, because the elevated number of pilot points from 14 to 94 brings more information from hydraulic head data. From Case 5 to Case 6, the number of pilot point is further increased from 94 to 494, but the ensemble mean and ensemble variance keep the same pattern and uncertainty. This means that additional information from pilot points can not improve the estimation and accuracy. In contrast, the elevated number of pilot points may introduce noises for individual realizations after interpolating by DS in Case 6.

For Case 7, we increased the ensemble size from 200 in Case 6 to 500 in Case 7, in order to improve
the quality of interpolated conductivity realizations. Ensemble mean and ensemble variance are smoothed
because cross-covariances are more accurately estimated with the larger ensemble size in the iterative ES.
This is consistent with studies of data assimilation via the EnKF (e.g., Hendricks Franssen and Kinzelbach,
2009).

Figure 8 displays the histogram of log-conductivity for Cases 3, 5 and 6. It is evident that, if iterative ES is used alone, the updated conductivity is inclined to be Gaussian, however, when iterative ES is coupled with DS via pilot points, the bimodal distribution of log-conductivity, as shown in the reference field, can be preserved after conditioning on hydraulic head data using the proposed approach.

204 4.2. Hydraulic Head

Besides looking at the characterization of conductivity, the reproduction of hydraulic head can also be 205 used to validate the methodology. Recall piezometric head data from Well #1-#9 are integrated into the groundwater flow model for calibrating conductivities. Figure 9 shows the simulated heads for the first 6 Cases 207 for well #6. With conditioning on measured conductivities, the uncertainty of simulated heads is reduced 208 from Case 1 to Case 2. With the best estimation of conductivity in Case 6 using an ensemble size of 200, the reference head is close to the mean of simulated heads and the spread of simulated heads is the smallest one 210 within the first 6 Cases. This result is consistent with the characterization of hydraulic conductivity. Note 211 that the capability of reproducing the reference head depends on how much information/data are considered 212 and integrated into the model. In these Cases, only 9 measured conductivities and head data from 9 wells are used to characterize complex patterns that display a high non-Gaussianity. The overall uncertainty of 214 simulated heads still shows a high uncertainty, as expected, based on Bayes' rule. If additional data such as measured conductivities and head data are conditioned further using the proposed approach, its uncertainty will certainly reduced.

4.3. Transport Prediction

218

The main purpose of data assimilation is to improve the predictive capability of the flow and transport model. The solute migration is more sensitive to preferred flow paths than hydraulic conductivity. In this work, a line of contaminant source with a constant concentration is released near the west boundary. The total simulation time for the transport migration is 1500 days and the start concentration is 30mg/l. Porosity is assumed to be 0.3. MT3D (Zheng and Wang, 1999) is used to solve the transport equation (2).

Figures 10 and 11 display the ensemble mean and ensemble variance of plume migration for 7 Cases
as well as the simulated plume for the reference conductivity field. The plume migration of the reference
conductivity field clearly shows channel structures which are propagated from the geologic structures of
conductivities. When including measured conductivities and head data, the reproduction of plume migration
to the reference one is the best. In this work, only hydraulic head data collected from 9 monitoring wells are
used for conditioning. If concentration data are sampled and used for conditioning as well, the prediction of
plume migration will be considerably improved, as it was demonstrated in Li et al. (2012).

5. Conclusion

In this paper, a new approach to assimilate dynamic data into a non-Gaussian aquifer by coupling the 232 iterative Ensemble Smoother and multiple-point geostatistics method is proposed. It borrows the advantages 233 of both DS method in modeling non-Gaussianity and iES in assimilating dynamic data. This new method 234 is aimed at reproducing channelized structures by assimilating indirect data such as hydraulic head. A 235 synthetic study has been applied to test the capability of the new approach. Seven Cases are conducted to 236 evaluate this new method. Among the seven Cases, the sensitivity of the number of pilot points and ensemble 237 size to the results are evaluated. The results show that, after combining DS method and iterative ES through 238 pilot points, hydraulic head data can be successfully assimilated into the non-Gaussian aquifer as well as 239 preserving the bimodal distribution that is displayed in the conceptual model (i.e., training image). The 240 coupled iES-DS has a better performance than iES alone since iES is not be able to keep the non-Gaussian distribution because of the use of two-point statistics for estimating correlations between state variables 242 and parameters. Flow and transport predictions are then introduced to test the predictive capability of 243 the updated conductivities. The results show that it can give a better prediction on both hydraulic head

- and contaminant transport, after all the data are integrated into the model, and more importantly, the non-Gaussian feature is preserved after assimilating dynamic data. The proposed iES-DS method provides a new avenue for groundwater inverse modeling in a non-Gaussian aquifer.
- Acknowledgements. The first author acknowledges the financial support of the South Dakota Board of
- 249 Regents through a Competitive Research Grant. The authors also wish to thank the associate editor and
- 250 two anonymous reviewers for their comments, which substantially helped to improve the final version of the
- 251 manuscript.

252 References

- Bailey, R., Baù, D., 2010. Ensemble smoother assimilation of hydraulic head and return flow data to estimate
 hydraulic conductivity distribution. Water Resources Research 46 (12).
- Bailey, R. T., Baù, D. A., Gates, T. K., 2012. Estimating spatially-variable rate constants of denitrification in irrigated agricultural groundwater systems using an ensemble smoother. Journal of hydrology 468,
- ₂₅₇ 188–202.
- 258 Bear, J., 1972. Dynamics of fluids in porous media. American Elsevier Pub. Co., New York.
- ²⁵⁹ Caers, J., 2003. History matching under training-image-based geological model constraints. SPE Journal 8 (11), 218–226.
- ²⁶¹ Chen, Y., Zhang, D., 2006. Data assimilation for transient flow in geologic formations via ensemble kalman ²⁶² filter. Advances in Water Resources 29 (8), 1107–1122.
- De Marsily, G., Delay, F., Goncalves, J., Renard, P., Teles, V., Violette, S., 2005. Dealing with spatial heterogeneity. Hydrogeology Journal 13 (1), 161–183.
- Deutsch, C. V., Journel, A. G., 1992. GSLIB, Geostatistical Software Library and User's Guide. Oxford
 University Press, New York.
- Emerick, A. A., Reynolds, A. C., 2013. Ensemble smoother with multiple data assimilation. Computers & Geosciences 55, 3–15.
- Evensen, G., 1994. Sequential data assimilation with a nonlinear quasi-geostrophic model using monte carlo methods to forecast error statistics. Journal of Geophysical Research: Oceans 99 (C5), 10143–10162.

- Gómez-Hernández, J. J., Journel, A. G., 1993. Joint sequential simulation of multigaussian fields. In: Geostatistics Troia92. Springer, pp. 85–94.
- Gomez-Hernandez, J. J., Sahuquillo, A., Capilla, J., 1997. Stochastic simulation of transmissivity fields
 conditional to both transmissivity and piezometric data i. theory. Journal of Hydrology 203 (1-4), 162–
- 275 174.
- Gu, Y., Oliver, D. S., et al., 2005. History matching of the punq-s3 reservoir model using the ensemble kalman filter. SPE journal 10 (02), 217–224.
- Harbaugh, A. W., Banta, E. R., Hill, M. C., McDonald, M. G., 2000. MODFLOW-2000, the U.S. Geological
- Survey modular ground-water model. U.S. Geological Survey, Branch of Information Services, Reston, VA,
- Denver, CO.
- Hendricks Franssen, H., 2001. Inverse stochastic modelling of groundwater flow and mass transport. Ph.D.
- thesis, Technical University of Valencia.
- ²⁸³ Hendricks Franssen, H., Alcolea, A., Riva, M., Bakr, M., van der Wiel, N., Stauffer, F., Guadagnini, A.,
- 2009. A comparison of seven methods for the inverse modelling of groundwater flow. application to the
- characterisation of well catchments. Advances in Water Resources 32 (6), 851–872.
- Hendricks Franssen, H. H., Kinzelbach, W., 2009. Ensemble kalman filtering versus sequential self-calibration
- for inverse modelling of dynamic groundwater flow systems. Journal of Hydrology 365 (3), 261–274.
- Hu, L. Y., 2000. Gradual deformation and iterative calibration of gaussian-related stochastic models. Math-
- ematical Geology 32 (1), 87–108.
- Huang, C., Hu, B. X., Li, X., Ye, M., 2009. Using data assimilation method to calibrate a heterogeneous con-
- ductivity field and improve solute transport prediction with an unknown contamination source. Stochastic
- Environmental Research and Risk Assessment 23 (8), 1155.
- ²⁹³ Kurtz, W., Hendricks Franssen, H.-J., Kaiser, H.-P., Vereecken, H., 2014. Joint assimilation of piezometric
- heads and groundwater temperatures for improved modeling of river-aquifer interactions. Water Resources
- 295 Research 50 (2), 1665–1688.
- Lengler, U., De Lucia, M., Kühn, M., 2010. The impact of heterogeneity on the distribution of co2: Numerical
- simulation of co2 storage at ketzin. International Journal of Greenhouse Gas Control 4 (6), 1016–1025.

- Li, L., Puzel, R., Davis, A., 2018a. Data assimilation in groundwater modelling: ensemble kalman filter versus ensemble smoothers. Hydrological Processes 32 (13), 2020–2029.
- Li, L., Srinivasan, S., Zhou, H., Gómez-Hernández, J. J., 2013. Simultaneous estimation of geologic and reservoir state variables within an ensemble-based multiple-point statistic framework. Mathematical Geosciences 46 (5), 597–623.
- Li, L., Srinivasan, S., Zhou, H., Jaime Gomez-Hernandez, J., 2015. Two-point or multiple-point statistics?

 a comparison between the ensemble kalman filtering and the ensemble pattern matching inverse methods.

 Advances in Water Resources 86, 297–310.
- Li, L., Stetler, L., Cao, Z., Davis, A., 2018b. An iterative normal-score ensemble smoother for dealing with non-gaussianity in data assimilation. Journal of Hydrology.
- Li, L., Zhang, M., Katzenstein, K., 2017. Calibration of a land subsidence model using insar data via the ensemble kalman filter. Ground Water 55 (6), 871–878.
- Li, L., Zhou, H., Gómez-Hernández, J. J., Franssen, H.-J. H., 2012. Jointly mapping hydraulic conductivity and porosity by assimilating concentration data via ensemble kalman filter. Journal of hydrology 428, 152–169.
- Liu, G., Chen, Y., Zhang, D., 2008. Investigation of flow and transport processes at the made site using ensemble kalman filter. Advances in Water Resources 31 (7), 975–986.
- Mariethoz, G., Renard, P., Straubhaar, J., 2010. The direct sampling method to perform multiple-point geostatistical simulations. Water Resources Research 46 (11).
- Oliver, D., Cunha, L., Reynolds, A., 1997. Markov chain Monte Carlo methods for conditioning a permeability field to pressure data. Mathematical Geology 29 (1), 61–91.
- Rabideau, A. J., Miller, C. T., 1994. Two-dimensional modeling of aquifer remediation influenced by sorption nonequilibrium and hydraulic conductivity heterogeneity. Water Resources Research 30 (5), 1457–1470.
- RamaRao, B. S., LaVenue, A. M., De Marsily, G., Marietta, M. G., 1995. Pilot point methodology for automated calibration of an ensemble of conditionally simulated transmissivity fields: 1. theory and computational experiments. Water Resources Research 31 (3), 475–493.

- Reichle, R. H., McLaughlin, D. B., Entekhabi, D., 2002. Hydrologic data assimilation with the ensemble kalman filter. Monthly Weather Review 130 (1), 103–114.
- Sarma, P., Chen, W. H., et al., 2009. Generalization of the ensemble kalman filter using kernels for nongaussian random fields. In: SPE reservoir simulation symposium. Society of Petroleum Engineers.
- Strebelle, S., 2002. Conditional simulation of complex geological structures using multiple-point statistics.

 Mathematical Geology 34 (1), 1–21.
- van Leeuwen, P. J., Evensen, G., 1996. Data assimilation and inverse methods in terms of a probabilistic formulation. Monthly Weather Review 124 (12), 2898–2913.
- Xu, T., Gómez-Hernández, J. J., Zhou, H., Li, L., 2013. The power of transient piezometric head data in inverse modeling: An application of the localized normal-score enkf with covariance inflation in a heterogenous bimodal hydraulic conductivity field. Advances in water resources 54, 100–118.
- Yeh, W., 1986. Review of parameter identification procedures in groundwater hydrology: The inverse problem. Water Resources Research 22 (2), 95–108.
- Zheng, C., Wang, P. P., 1999. MT3DMS: A Modular Three-Dimensional Multispecies Transport Model for
 Simulation of Advection, Dispersion, and Chemical Reactions of Contaminants in Groundwater Systems;
 Documentation and User's. ALABAMA UNIV TUSCALOOSA.
- Zhou, H., Gómez-Hernández, J. J., Hendricks Franssen, H.-J., Li, L., 2011. An approach to handling non gaussianity of parameters and state variables in ensemble kalman filtering. Advances in Water Resources
 34 (7), 844–864.
- Zhou, H., Gómez-Hernández, J. J., Li, L., 2012. A pattern-search-based inverse method. Water Resources
 Research 48 (3).
- Zhou, H., Gomez-Hernandez, J. J., Li, L., 2014. Inverse methods in hydrogeology: Evolution and recent
 trends. Advances in Water Resources 63, 22–37.

Table 1: Setup of the groundwater flow model

Training image size	250×250
Model size	50×50
Grid size	$5~\mathrm{m} \times 5~\mathrm{m}$
Aquifer thickness	$5 \mathrm{m}$
Simulation time	30 days
Number of periods	1
Number of time steps	60
Aquifer storage coefficient	0.003
Initial head	5 m

Table 2: Case study

	Case 1	Case 2	Case 3	Case 4	Case 5	Case 6	Case 7
Conditioned K	0	6	6	6	6	6	6
Conditioned h	0	0	9	9	9	9	9
Number of pilot points	0	0	0	14	94	494	494
Method	DS	DS	iES	iES-DS	iES-DS	iES-DS	iES-DS
Ensemble size	200	200	200	200	200	200	500

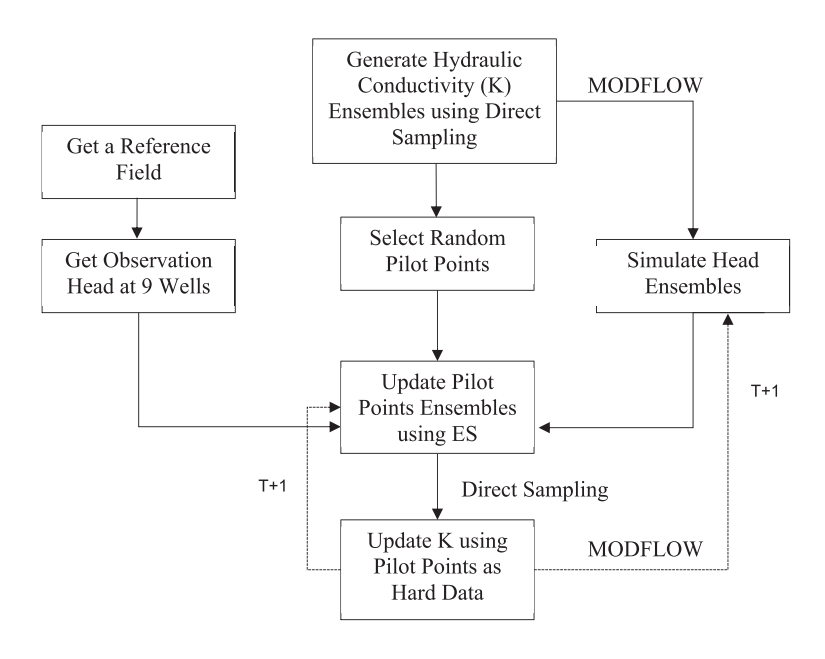


Figure 1: Flowchart of the proposed iES-DS method. First, a reference hydraulic conductivity field is generated as the 'true' one for validation. Then, the simulated head will be selected at 9 wells as observation data. DS is applied to generate hydraulic conductivity ensemble. The corresponding hydraulic head ensemble will be simulated by running MODFLOW and a certain number of pilot points will be selected randomly. The iterative ES is used to update conductivities at pilot points by integrating the head data collected from 9 wells. The updated conductivities at pilot points will be regarded as hard data to interpolate hydraulic conductivity field by DS. The updated conductivity fields will be used as the input for the next iteration until a convergence is achieved. T denotes the iteration number.

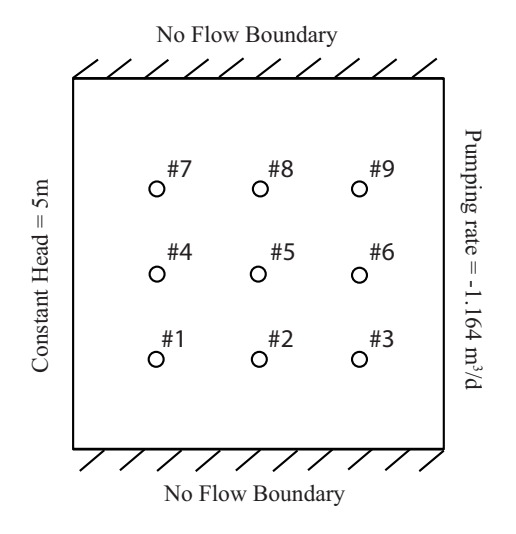


Figure 2: Boundary conditions and well locations.

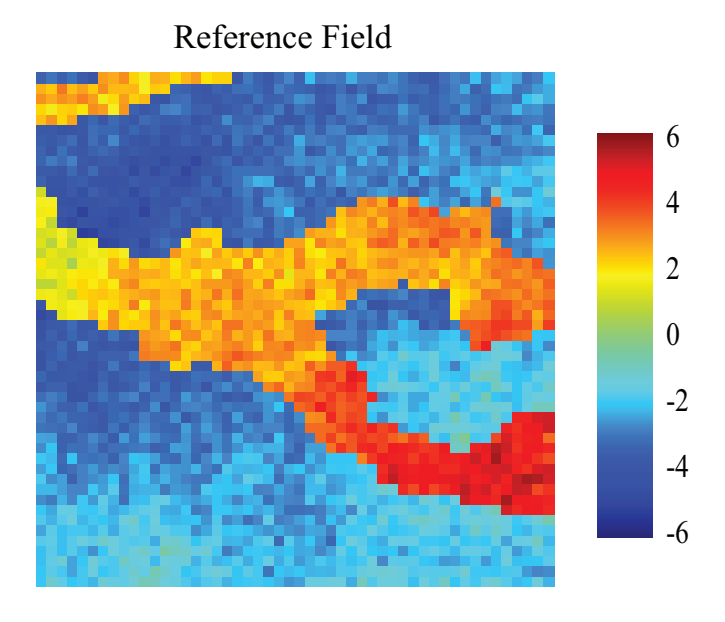


Figure 3: Reference log-conductivity field generated by Direct Sampling.

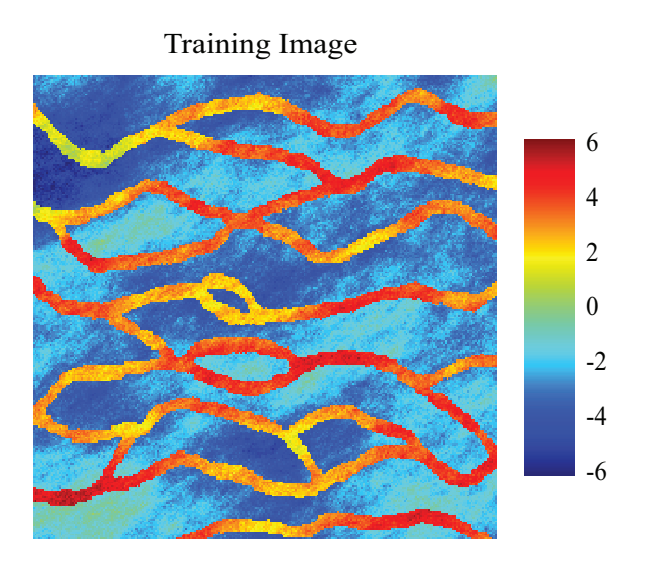


Figure 4: Training image generated by overlaying a continuous conductivity field on a categorical facies field.

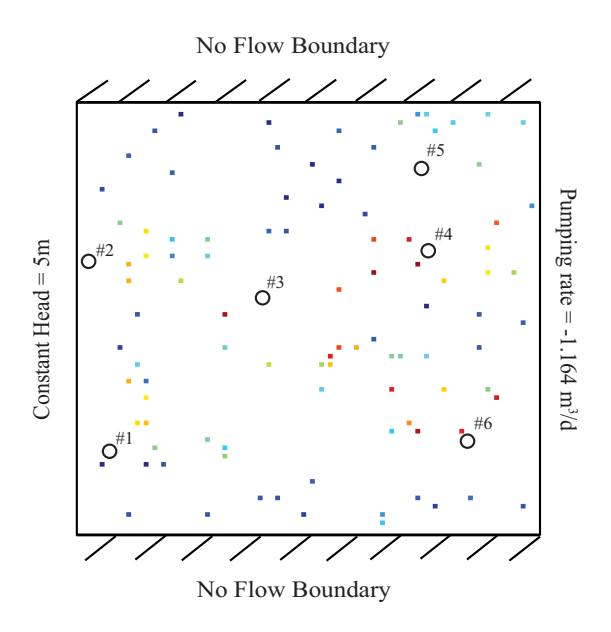


Figure 5: The distribution of pilot points. The color dots are pilot points and the white circles are measured conductivities

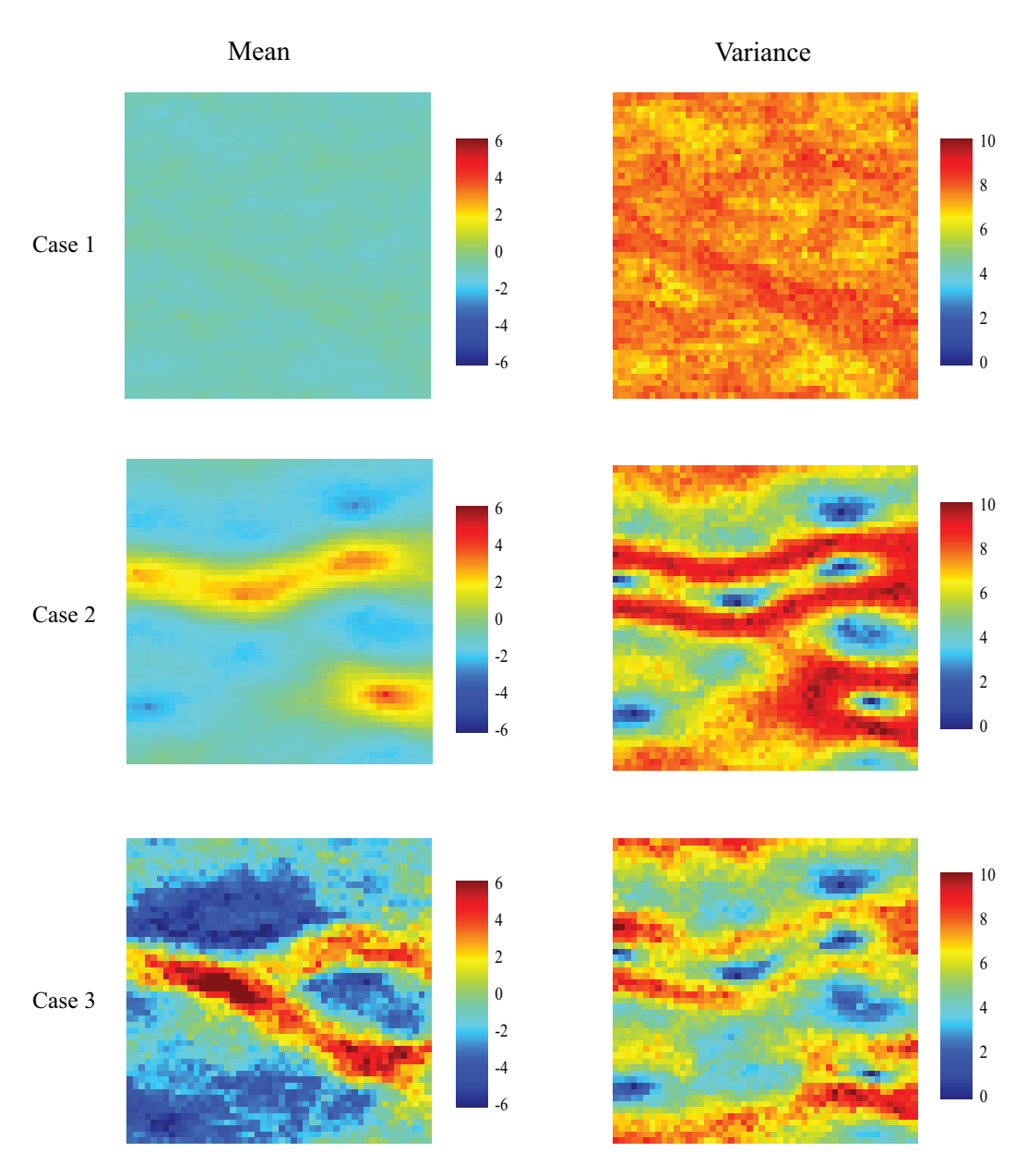


Figure 6: Ensemble mean and ensemble variance for case 1-3.

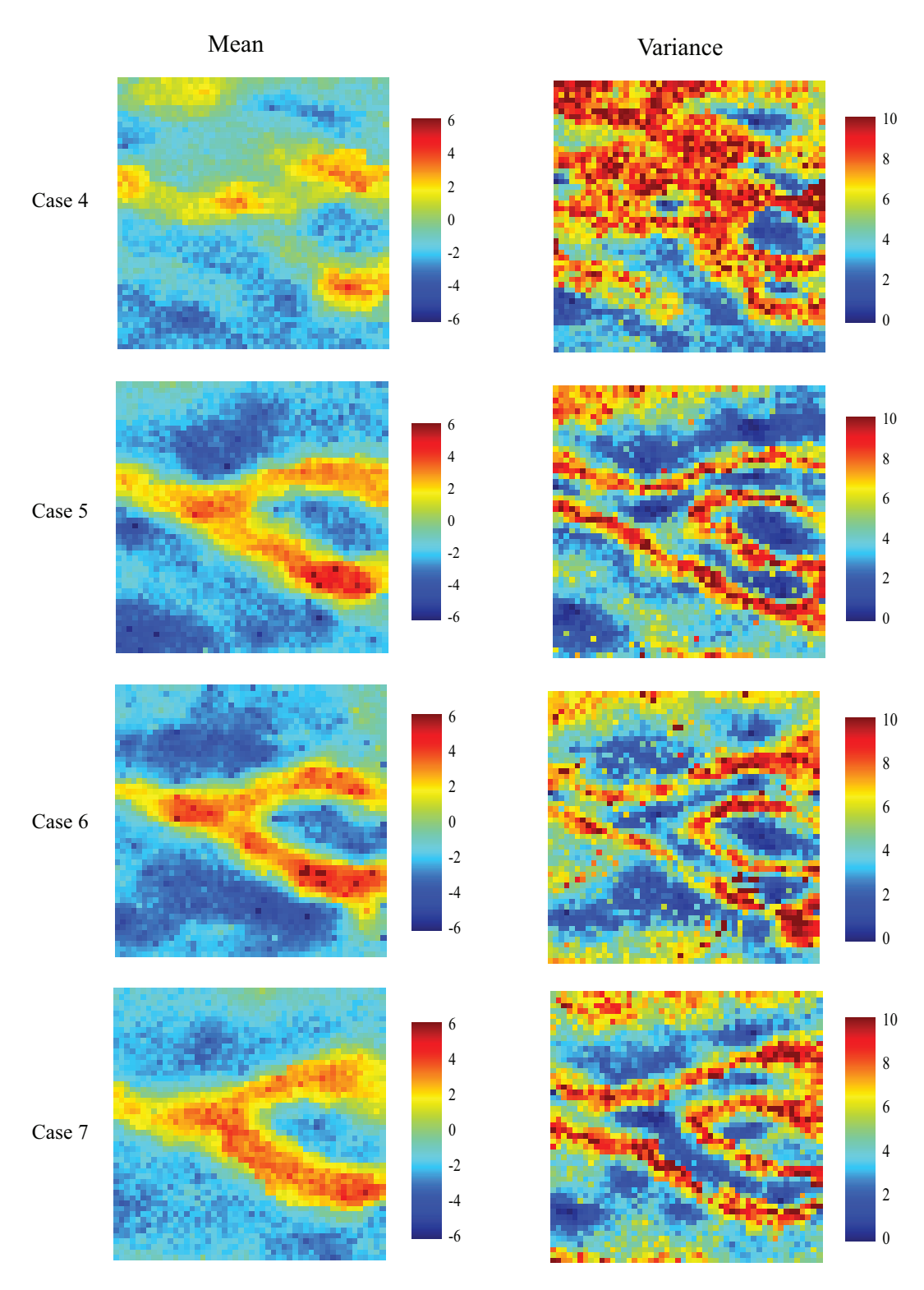


Figure 7: Ensemble mean and ensemble variance for case 4-7.

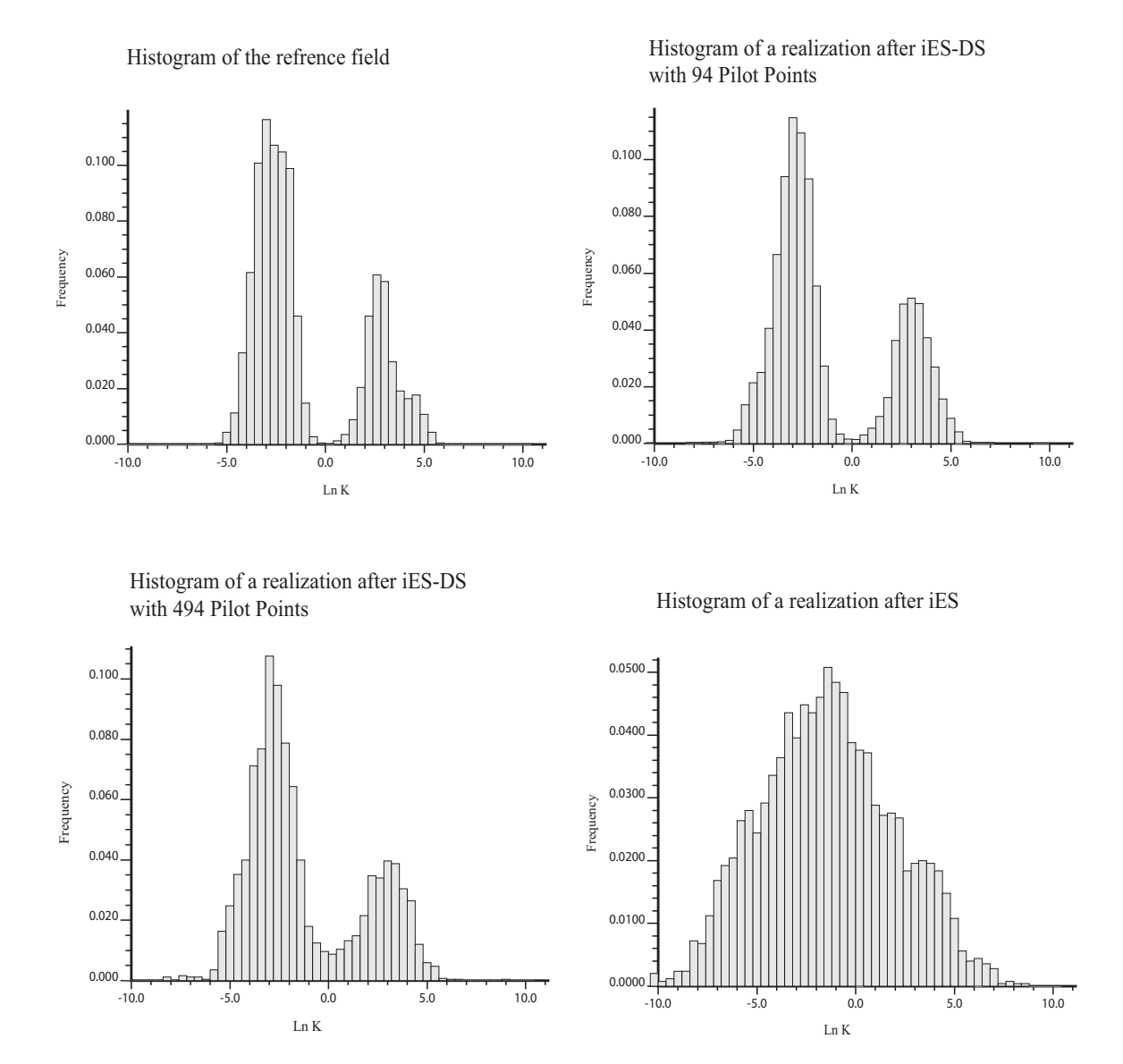


Figure 8: Histogram of log-conductivity for difference cases.

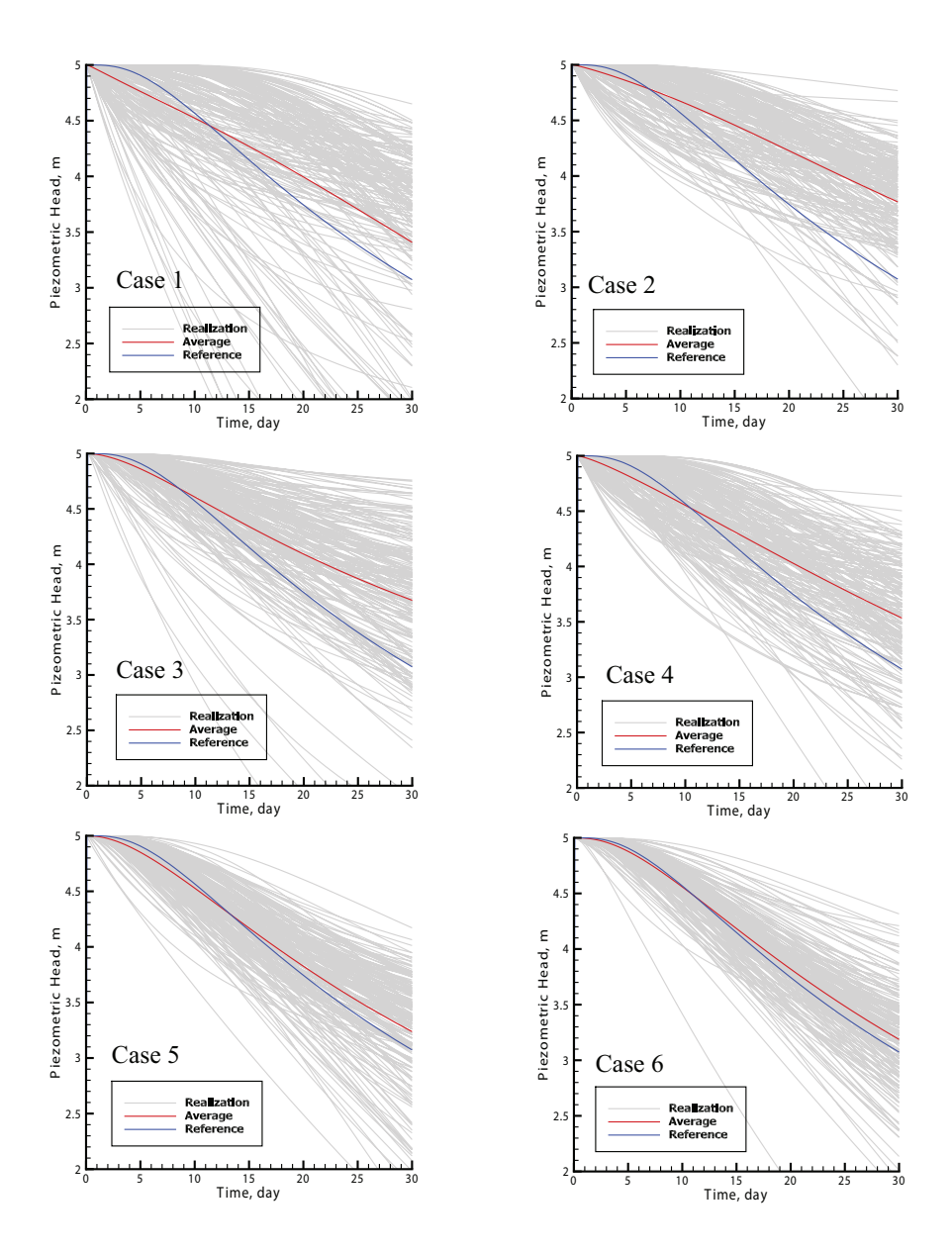


Figure 9: Flow prediction at well #6 .

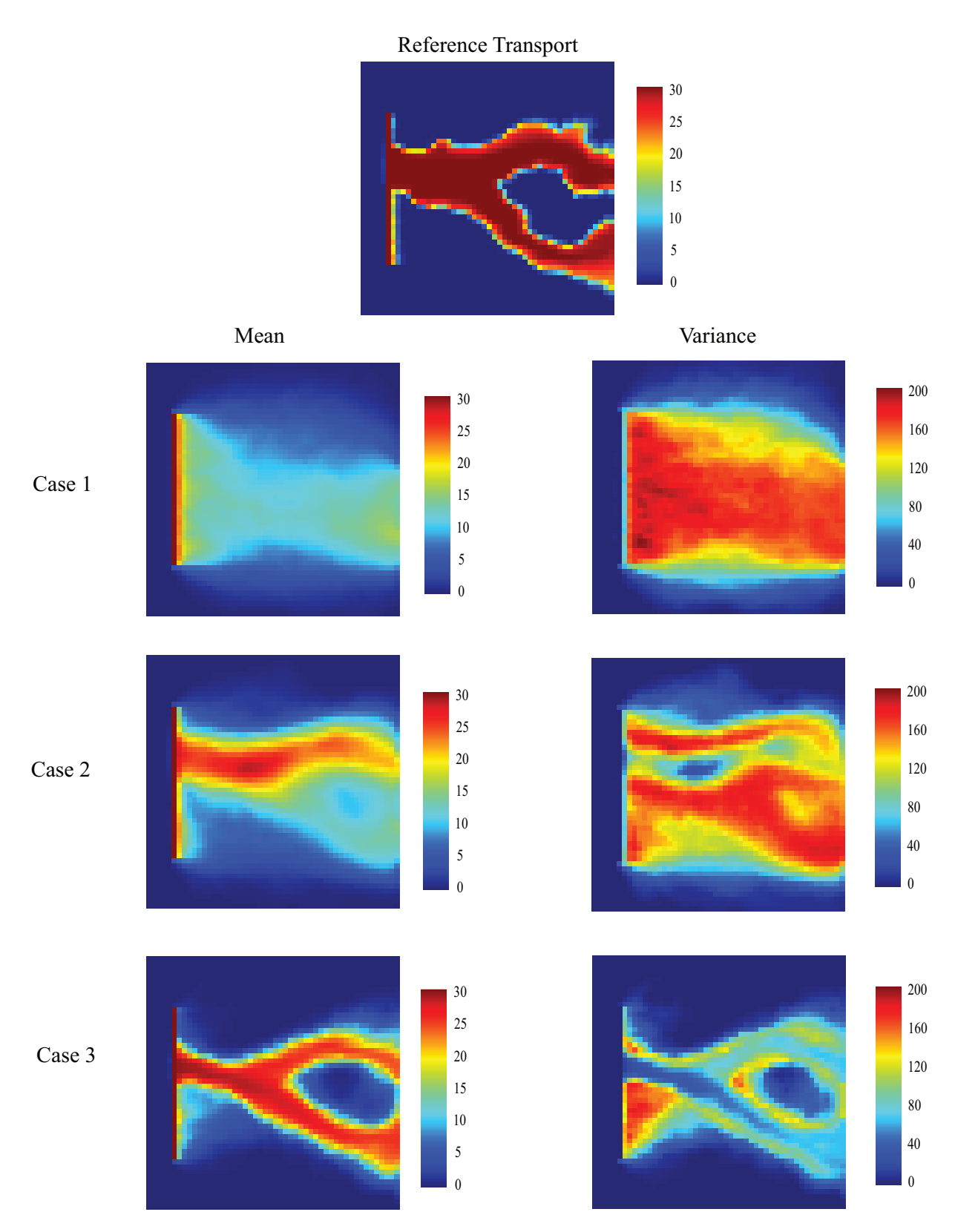


Figure 10: Ensemble mean and ensemble variance of transport migration for Case 1-3.

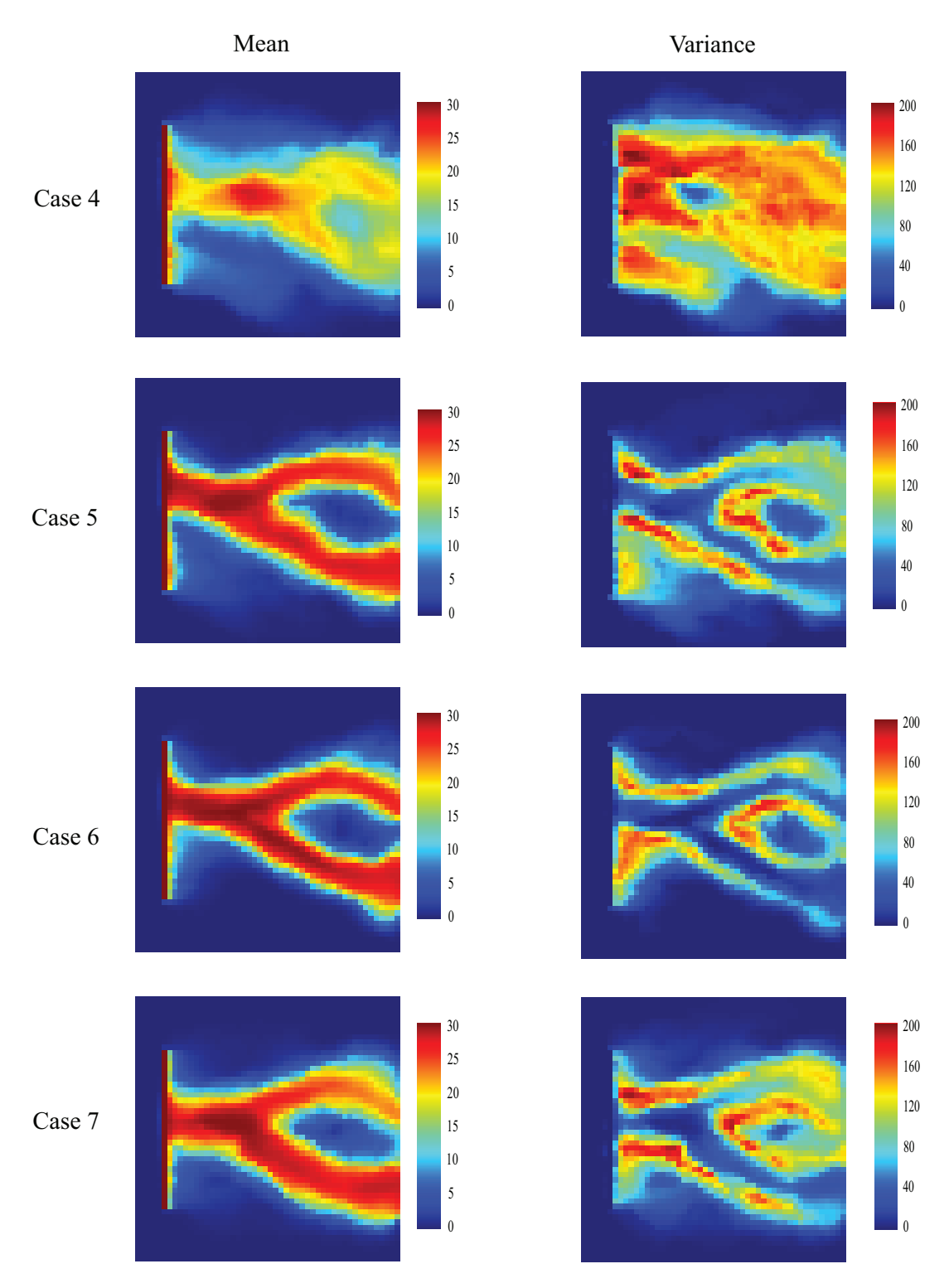


Figure 11: Ensemble mean and ensemble variance of transport migration for Case 4-7.